Improved Microstrip Folded Tri-Section Stepped Impedance Resonator Bandpass Filter using Defected Ground Structure

Nima Molaei Garmjani and Nader Komjani

Department of Electrical Engineering
Iran University of Science & Technology (IUST), Tehran, Iran
nima_molaei@yahoo.com, n_komjni@iust.ac.ir

Abstract ─ In this paper, a study of a microwave microstrip bandpass filter (BPF), based on folded tri-section stepped impedance resonator (FTSIR) and defected ground structure (DGS) is presented. Based on the resonance characteristics of a stepped impedance resonator (SIR), the first spurious resonant frequency can be tuned over a wide range by adjusting its structure parameters. The SIR bandpass filter is designed to have a quasi-elliptic function response and a wide upper stopband. Furthermore, five ground slots (DGS) are used in order to omit the first spurious resonant frequency. Compared to similar microstrip filter without defected ground, the simulated performances of this novel structure indicate some functional advantages. To validate the design and analysis, a prototype of the bandpass filter with DGS was fabricated and measured. It is shown that the measured and simulated performances are in a good agreement.

Index Terms ─ Defected ground structure (DGS), folded tri-section stepped impedance resonator (FTSIR), microstrip bandpass filter.

I. INTRODUCTION

By using a SIR the first and second spurious response can be pushed far beyond $2f_0$ and $3f_0$, respectively (where f_0 is the fundamental resonant frequency); this is achieved by properly choosing the impedance ratio. In addition, bandpass filters based on stepped impedance resonators usually have high selectivity and low internal losses in pass band width. For this reason, these filters are extensively used in a most of the communication applications nowadays. Stepped impedance resonators are use in circuits like duplexers and mixers because they have smaller dimensions, relative to conventional resonators, and high quality factor.

There are many types of transfer functions for filters (Butterworth, Chebyshev, Elliptic, Quasi-elliptic, etc.). Among these different types, filters with quasi-elliptic transfer function have higher selectiveness, because of having the same ripples in pass band and high slope nearby transmission zeros. In addition, the ability to create transfer zeros in nearby of pass band causes to improve the slope of reject band. So, quasi-elliptic filters are extensively used in modern applications.

Poles degree of the filter and consequently the quantity of resonators must be increased in order to obtain higher selectiveness, but internal losses increase because resonators are not ideal. Here, in the design process of SIR filters, we have used quasi-elliptic four-pole cross-coupled resonators (reciprocal coupling between nonadjacent resonators) in order to obtain high selectiveness and decrease the internal loss. Whereas the first spurious resonant frequency is near to pass band in this structure, we have to consider an approach to eliminate it. The selected approach to eliminate the first spurious resonant frequency is etching defects in the ground plane of the structure.

In [1], a FTSIR bandpass filter is designed, but here we will use a different structure and designing method; also, we will discuss the DGS design process in detail.

II. QUASI-ELLIPTIC BANDPASS FILTER BASED ON SIR

We used folded tri-section stepped impedance resonators to design a four-pole quasi-elliptic bandpass filter. The basic structure of tri-section SIR is shown in Fig. 1(a). The folded SIR is also shown in Fig. 1(c). These resonators not only have

smaller dimensions but also have wider rejection bandwidth comparing to other popular resonators.
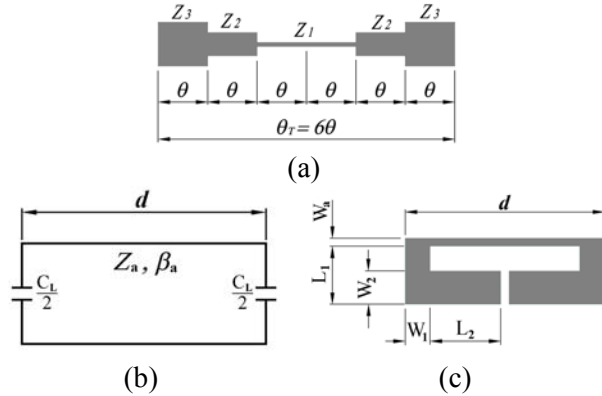

Fig. 1. (a) Basic structure of tri-section SIR resonator. (b) An equivalent circuit of proposed SIR resonator. (c) Proposed folded SIR resonator.

At first, let us consider a capacitively loaded lossless transmission line resonator of Fig. 1(b). C_L, Z_a, β_a, and d represent the loaded capacitance, the characteristic impedance, the propagation constant, and the length of the unloaded line, respectively. Thus, the electric length is $\theta_a = \beta_a d$. The related equations of folded SIR are derived in [1] and [2], such that:

$$\begin{cases} \theta_{a0} = 2\tan^{-1}\left(\dfrac{1}{\pi f_0 Z_a C_L}\right) \\ \theta_{a1} = 2\pi - 2\tan^{-1}\left(\pi f_1 Z_a C_L\right) \end{cases} \quad . \tag{1}$$

The fundamental resonant frequency and the first spurious resonant frequency are f_0 and f_1, respectively. If C_L equals to zero in the above equation, then θ_{a0} and θ_{a1} equals to π and 2π, respectively. If $C_L \neq 0$, the resonant frequencies shift down as the loaded capacitance increases.

Here, we have assumed $Z_a = 50\,\Omega$, $d = 18.15\,mm$, $W_a = 0.71\,mm$, $V_{Pa} = 1.149 \times 10^8\ m/s$ and V_{Pa} is associated phase velocity. We considered a Rogers RT/duroid 3010 substrate to design our filter; the substrate has a relative dielectric constant of 10.2, a thickness of 0.635 mm and a loss tangent of 0.0035.

The resonator of Fig. 1(c), which is composed of a microstrip line with both ends loaded with folded open-stubs, is used. The folded arms of open-stubs are applied for increasing the loading

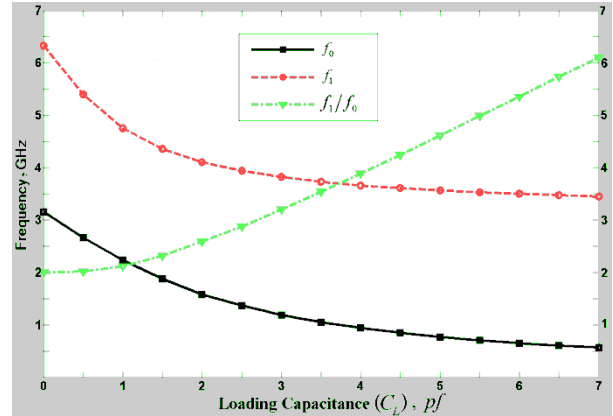capacitance to ground for the purpose of cross coupling.

Fig. 2. The fundamental, first spurious resonant frequencies and their ratio versus the loading capacitances.

According to (1), Fig. 2 plots the calculated resonant frequencies, as well as their ratio for different capacitance loading with the above mentioned values. As can be seen when the loading capacitance is increased, in addition to the decrease of both resonant frequencies, the ratio of the first spurious resonant frequency to the fundamental one is increased.

Shown in Fig. 2 are the fundamental and first spurious resonant frequencies as well as their ratio against the loading capacitances, obtained using a full-wave advanced design system (ADS) simulator. According to this Fig, the ratio of the first spurious resonant frequency to the main resonant frequency has direct relation to the loading capacitance. Increasing of the loading capacitance will increase the ratio of the first spurious resonant frequency to the main resonant frequency but the main and the first spurious resonant frequencies will decrease. It is possible to increase the distance between the first spurious and the main resonant frequencies by increasing the loading capacitance. This improves the filter characteristics in rejection band.

Figure 3 shows the fundamental and spurious resonant frequencies together with their ratio versus the length of folded open-stubs. The length of folded open-stubs (L) is obtained from [2]:

$$\begin{cases} L = L_1 & for \quad L \leq 6.5\ mm \\ L = 6.5 + L_2 & for \quad L > 6.5\ mm \end{cases} . \tag{2}$$
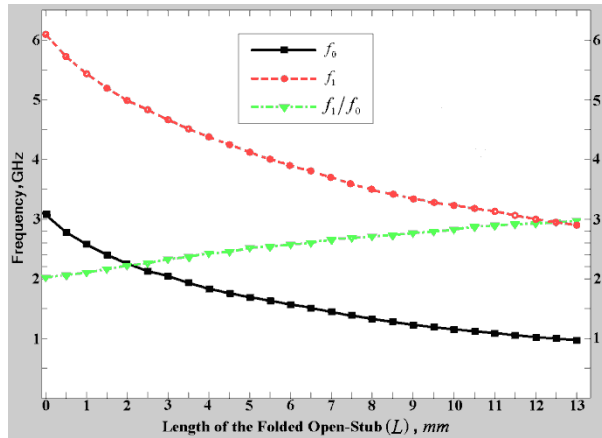
Fig. 3. The fundamental, spurious resonant frequencies and their ratio versus the length of the folded open-stub.

The increase profile of the ratio of the first resonant frequency to the main resonant frequency with the increase of L is similar to the increasing profile of this ratio with C_L. This matter was predictable because both graphs are discussing about an unloaded microstrip line width 18.15 mm length and 0.71 width which exists on a substrate with a relative dielectric constant of 10.2 and a thickness of 0.635 mm, only the open stub of the resonator of Fig. 3 is approximated by a capacitance (Fig. 2). It is important to say that the open-stub should have a wider line or lower characteristic impedance. In this case, according to Fig. 1(c), we have $W_1 = 2$ mm and $W_2 = 3.66$ mm for the folded open-stub.

To achieve high selectiveness, the order of filter must increase for the Butterworth and Chebyschev filters. Elliptic filter has ripple in the both pass band and rejection band due to having limited transmission zeroes; as a result, it is highly selective and its slope is much more than the above two filters. However, the realization of this type of filter with the printed circuits structure is complicated. The four-pole cross-coupled SIR filter is designed using the proposed basic resonator structure [3].

Figure 4 shows the arrangement of resonators in the quasi-elliptic four-pole SIR filter. Referring to Fig. 4, the coupling between resonators 1 and 4 is of electric type, between 2 and 3 is of magnetic type and between 1 and 2 is of mixed type as well as 3 and 4. More details about electric, magnetic,

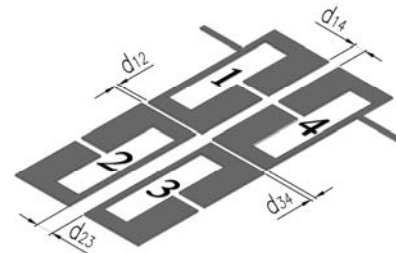and mixed coupling between the resonators are discussed in [2].

Fig. 4. Schematic of a quasi-elliptic four-pole SIR filter.

In order to design a quasi-elliptic four-pole SIR filter, it is essential to characterize the coupling between adjacent resonators. Fig. 5 shows a typical graph of magnetic coupling between two SIRS's for a desired distance between them, in a certain frequency range. This graph is derived via simulation.
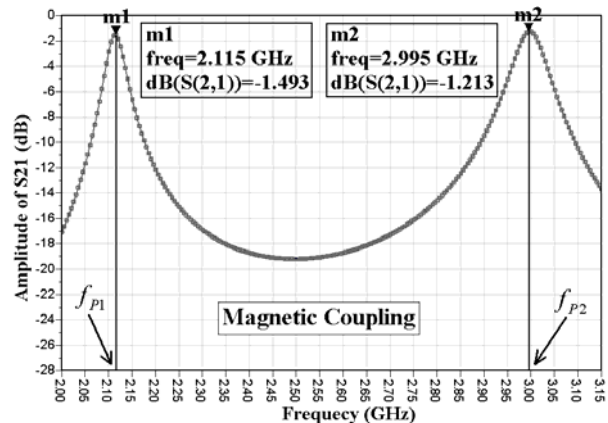

Fig. 5. Typical frequency responses simulated for extracting the coupling coefficient.

The coupling K_{ij} of any pair of adjacent SIR's is determined by [3].

$$K_{ij} = \frac{f_{P2}^2 - f_{P1}^2}{f_{P2}^2 + f_{P1}^2} . \qquad (3)$$

For the example in Fig. 5, the resonant frequencies f_{P1} and f_{P2} are obviously measurable based on amplitude frequency responses. In this sample, the values of resonant frequencies are $f_{P1} = 2.115$ GHz and $f_{P2} = 2.995$ GHz, so according to equation (2), we have:
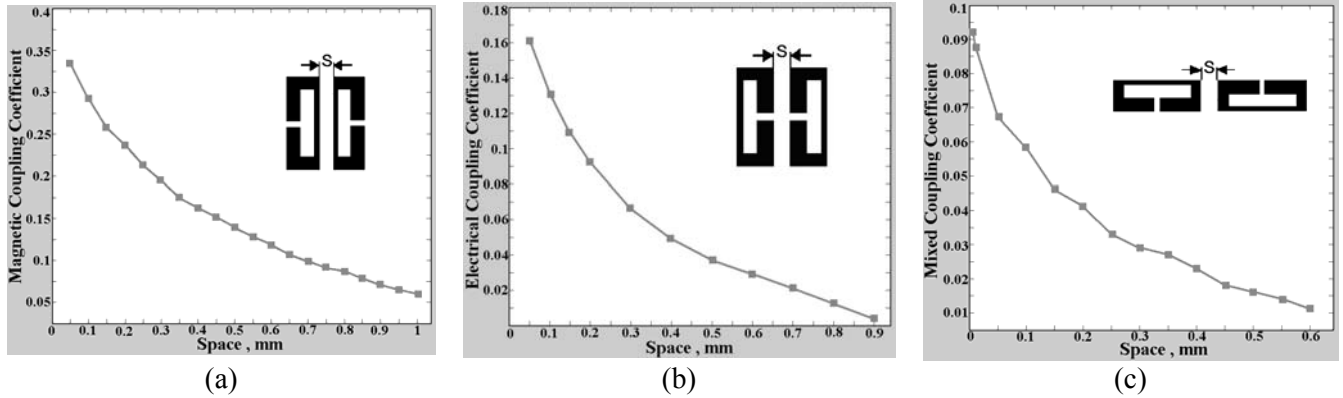
Fig. 6. Coupling coefficients against space between adjacent resonators (a) magnetic coupling, (b) electric coupling and (c) mixed coupling.

$$K_{23} = 0.334.$$

The graphs of coupling coefficient against space between adjacent resonators are derived according to equation (3) and Fig. 5 for three types of couplings which are used in the design of our filter. These graphs are shown in Fig. 6.

The equations for calculating coupling coefficient of different types of coupling may be obtained as described in [7]:

$$M_{14} = \frac{FBW \cdot J_1}{g_1}$$

$$M_{23} = \frac{FBW \cdot J_2}{g_2} \qquad (4)$$

$$M_{12} = M_{34} = \frac{FBW}{\sqrt{g_1 \, g_2}}.$$

The existing factors in (4) are specified for each certain filter characteristics in some tables which are presented in [4]. So the coupling coefficients of our desired filter may be obtained.

By using Fig. 6 spaces between each adjacent resonator may be obtained according to the above specified coupling coefficients. Our desired bandpass filter may be designed by this method.

Based on the substrate we selected, the design parameters of the resonator in Fig. 1(c) and the distance between the resonators of Fig. 4 are summarized in Table 1, with all dimensions shown in millimeters.

The results of the preliminary designed four-pole SIR filter are seen in Fig. 7. One can observe bandpass filter behaviour with central frequency of 0.965 GHz, and bandwidth of 85 MHz. The

insertion loss is, also, 1.55 dB and the return loss is better than 23 dB.

Table 1: The values of design parameters of the desired filter

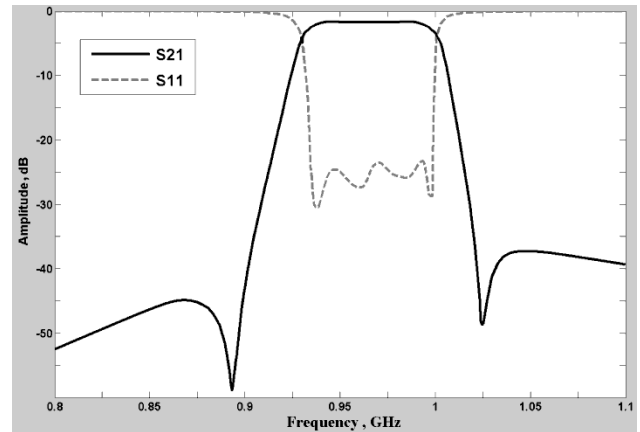| L_1	7.06	W_2	3.66	d_{14}	1.45
L_2	6.58	W_a	0.71	d_{23}	2.11
W_1	2.04	d	18.15	$d_{12} = d_{34}$	0.11

Fig. 7. Simulation of preliminary designed four-pole SIR filter.

Figure 8 shows the simulation results of the rejection band for the four-pole SIR filter. Referring to Fig. 8, the first spurious resonant frequency occurred at 3.2 GHz.

As can be seen, the rejection band width of the designed filter is almost short. Insertion loss at first spurious resonant frequency 3.2 GHz reaches to 5 dB. In order to improve the rejection band

width, we have to eliminate the first spurious frequency. To achieve this, we utilize the defected ground structures (DGS).
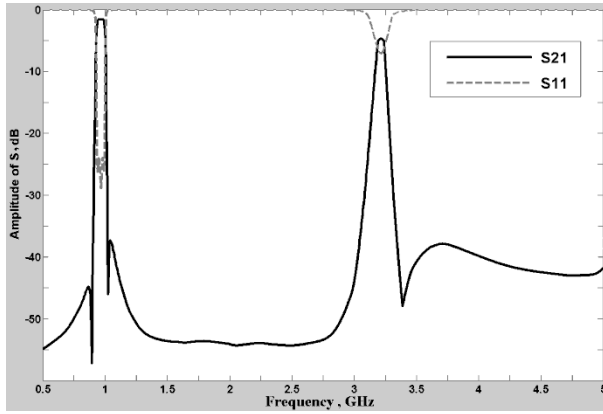

Fig. 8. Simulation of rejection band of the SIR filter.

III. DEFECTED GROUND STRUCTURE

Microstrips structures, with special shapes etched in their ground planes are one of the approaches that researchers use to improve the characteristics of filters. This generic structure is called defected ground structure (DGS). Some advantages of using DGS in filters are simple fabrication, the ability to transfer of high power, low insertion loss and minimization of the filter size. Among various suggested shapes of DGS structures is the rectangular structure due to its simplicity.

An LC equivalent circuit can represent the unit DGS circuit. The equivalent circuit parameters are affected by the physical dimensions of the DGS. The equivalent circuit and parameters of the DGS should be extracted in order to design a circuit with DGS section. One can derive the equivalent circuit of the DGS section using the ADS simulator. The equivalent inductive reactance can be easily calculated by using the prototype element value of the one-pole response.
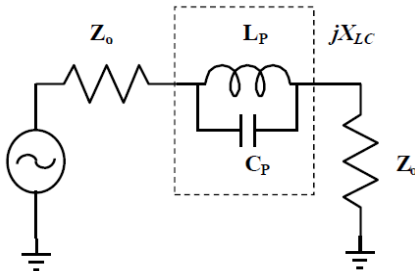

Fig. 9. Equivalent circuit of the DGS circuit.

The parallel capacitance value for the given DGS section can be extracted from the attenuation pole location frequency. The slot in ground plane excited by the microstrip line behaves as parallel resonance. Fig. 9 shows the equivalent circuit of the DGS circuit, where the dotted box shows the DGS section [5].

In Fig. 9, the parallel capacitance value C_P and the parallel inductance value L_P are as follows:

$$C_P = \frac{\omega_C}{Z_0\, g_1 \left(\omega_0^2 - \omega_C^2\right)} = \frac{5\, f_C}{\pi \left(f_0^2 - f_C^2\right)} \qquad pf\,, \qquad (5a)$$

$$L_P = \frac{250}{C_P \left(\pi f_0\right)^2} \qquad nH. \qquad (5b)$$

The equivalent reactance value for DGS unit can be expressed as below:

$$jX_{LC} = \frac{j\omega L_P \times \dfrac{1}{j\omega C_P}}{j\omega L_P + \dfrac{1}{j\omega C_P}} = \frac{j\omega L_P}{1 - \omega^2 L_P C_P} \qquad (6a)$$

$$\omega_0^2 = \frac{1}{L_P C_P} \qquad (6b)$$

$$X_{LC} = \frac{1}{\omega_0 C_P \left(\dfrac{\omega_0}{\omega} - \dfrac{\omega}{\omega_0}\right)}. \qquad (6c)$$

DGS structures etched under microstrip line increase the inductance and capacitance of line in the rejection band and this, consequently, decreases the propagation velocity. In this situation, the slots in the ground plane cause a portion of density of electrical flow to couple to the side line which in normal design it couples to the ground plane. This will increase the capacitance coupling in coupled lines. Also, because of the type of etched slot on the ground plane, phase velocity of the even and odd modes will be equal. By equalizing the even and odd mode phase velocities it is possible to suppress the first harmonic.

A. Rectangular slots in the direction of coupling line

According to Fig. 10, in this situation of arrangement of DGS unit in the ground plane of coupling lines, slots do not cause any changes in the field lines of the odd mode, but for the even mode, part of electrical field will propagate in the

space under the slot because of the distance between two DGS structures (S_M), Fig. 10 (b). This will decrease the effective relative dielectric coefficient in even mode (ε_{eff}^e) [6].
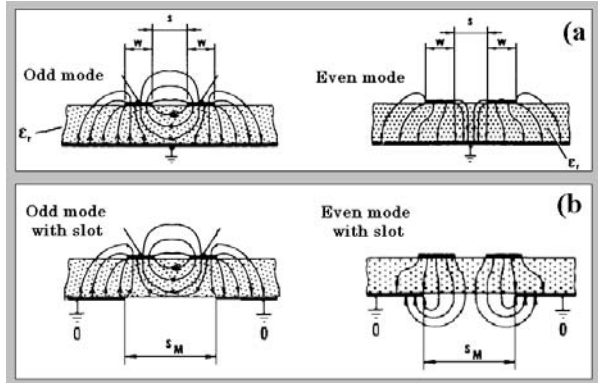

Fig. 10. (a) Electrical filed lines in odd and even modes, in structure of coupling lines without DGS. (b) Electrical filed lines in odd and even modes, in structure of coupling lines with DGS [6].

Etching a slot in a direction of the coupled lines decreases ε_{eff}^e and makes it closer in values to ε_{eff}^o (the effective relative dielectric coefficient in odd mode). As Fig. 10 shows, ε_{eff}^o does not change. So, the difference between phase velocity at even mode and odd mode ($\varepsilon_{eff}^{even} > \varepsilon_{eff}^{odd}$), which exists in normal design, will decrease and the phase velocity of the two modes will become approximately equal. Rectangular slots can be located in different positions in direction of coupling lines which will be discussed. Width, length and location of slots are the main design parameters which increase the coupling and equalize the phase velocity in odd and even modes.

To determine each one of these parameters, two other parameters should be considered as a constant and the influence of changes in the first one on the coupling will be studied. According to Fig. 11 among situations 1, 2, and 3, no. 1 is the most effective one on the coupling. Regarding the width of the slots, three different conditions will be discussed which have better performance than others [5]; first equal to the width of coupling line (W), second equal to the distance between coupling line (S), and third equal to the average of the last two ones (W+S/2). Among these three cases, the second one has the most degree of influence on the coupling. Regarding the effect of length of the slots on the coupling, there are three different options; first equal to half of the length of the coupling line, second equal to the length of the coupling line, and third equal to the total length of the ground plane. The last two options have more influence on coupling compared to the first one. It is notable that between these two, the length equal to the length of the coupling line is more common.

Situation no. 4 in Fig. 11 is a more effective structure to equalize the phase velocity of even and odd phases as well as having great influence on increasing the coupling like the previous study in [5].
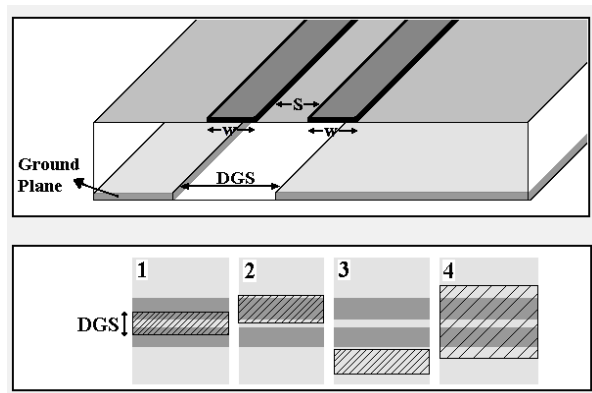

Fig. 11. Different situations of DGS location in ground plane of two coupling lines.

B. Rectangular slots perpendicular to the direction of coupling lines

In this situation, as shown in Fig 10(b), the electrical field lines are similar to the case without DGS; so ε_{eff}^o will not change. In even mode, the signal path increases for a special physical length due to the existence of the DGS in the ground plane. This increase in signal path is equal to the decrease of phase velocity in even mode. In other words, ε_{eff}^e and ε_{eff}^o increase equally. This increase of signal path is similar to the increase of return currents path in ground plane for a simple line with DGS.

In fact, the increase of ε_{eff}^e causes more difference between phase velocities in two modes. On the other hand, this increase of ε_{eff}^e and no change of ε_{eff}^o causes the coupling between the resonator lines to increase, compared to the case without DGS.

IV. IMPROVED MICROSTRIP SIR BANDPASS FILTER USING DEFECTED GROUND STRUCTURES

One method to improve the filter characteristics is to use microstrip structures with defected ground plane. DGS cells are used as complementary of the main filter and also independently in executing the filter, due to having natural resonant characteristics [5]. DGS structures generally affect the filter rejection band. The effects of these structures on improving the filter characteristic in pass band are also discussed. Easily fabrication, low insertion loss, and size reduction of the filters are some advantages of using DGS structure in design of filters [7].

In order to prevent radiation from DGS, we have to know distribution of surface currents on the ground plane of the filter which is shown in Fig. 12.
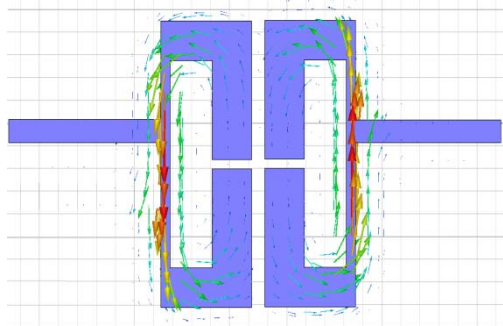

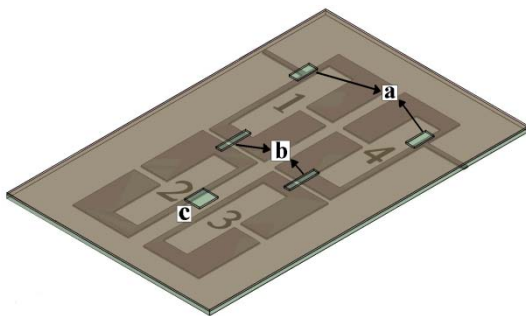Fig. 12. The distribution of surface currents on the ground plane of the filter.

Fig. 13. Schematic of designed four-pole SIR filter with DGS.

For realization of desired DGS structure, considering discussed issues in [7], we utilized a simple linear slot in the ground plane of the preliminary designed filter. Two simple linear slots are etched in the ground plane, one between resonators No. 1 and 2 and the other between resonators No. 3 and 4, in order to improve the mixed coupling between them. The other slots are applied to improve the coupling between the input and output of the filter.

Dimensions of the used DGS slots in Fig. 13 are identified in Table 2, with all dimensions shown in millimeters.

Table 2: Dimension of the DGS slots of Fig. 13

DGS	DGS Length	DGS Width
a	2.8	1.24
b	4.19	0.78
c	2.63	2.11

Figure 14 shows the simulation results of the passband for the four-pole SIR filter with DGS.
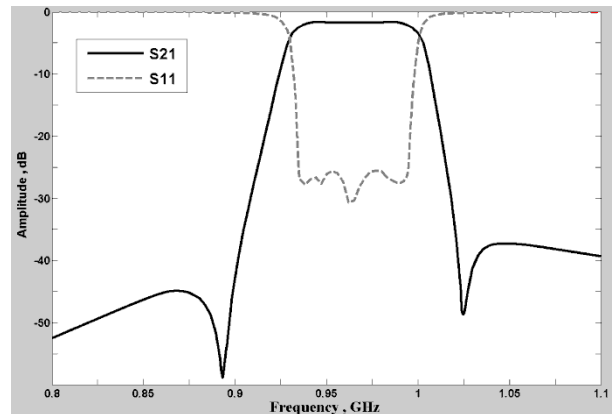

Fig. 14. Simulation results of the pass band for the improved four-pole SIR filter with DGS.
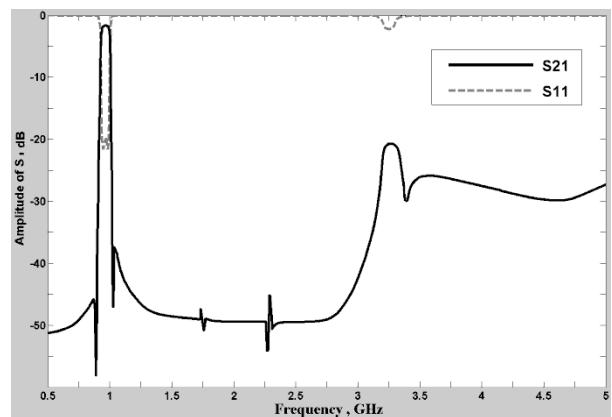

Fig. 15. Simulation results of the SIR filter with DGS in the range 0.5-5 GHz.

As observed in Fig. 14, insertion loss is 1.6 dB and return loss is better than 24 dB. The bandwidth of the filter reached to 85 MHz at 0.965

GHz central frequency which is in a good agreement with the case without DGS.

We can see 16 dB improvements in the insertion loss of the first spurious resonant frequency of the filter according to Fig. 15. In fact, insertion loss at 3.2 GHz reaches 21 dB. In addition, comparing the frequency response of the preliminary SIR filter (without DGS) to the SIR filter with DGS in Fig. 8, we observe elimination of the spurious frequency response in frequency 3.2 GHz. Frequency responses of the filter with and without DGS are compared in Table 3.

Table 3: Comparing the frequency responses of the filter with and without DGS

S parameter	Without DGS	With DGS
Insertion loss at the fundamental frequency (dB)	1.55	1.6
Return loss at the fundamental frequency (dB)	23	24
Insertion loss at the first spurious frequency (dB)	5	21

V. MEASURED RESULTS AND COMPARISON WITH SIMULATED

A sample of four-pole SIR bandpass filter with DGS was fabricated and measured. Photographs of the fabricated filter with DGS are shown in Fig. 16. The prototype circuit size of the filter is around 44.6 mm × 28.4 mm.
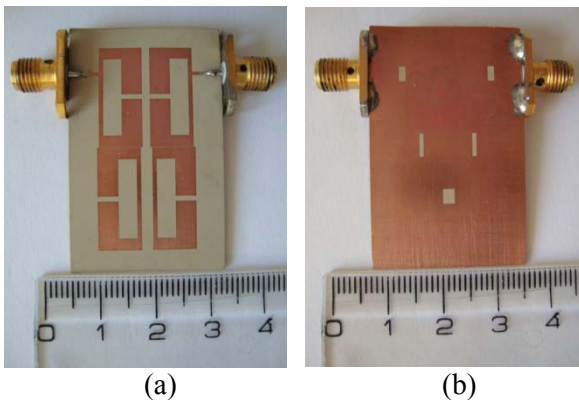

(a)   (b)

Fig. 16. Photograph of the fabricated four-pole SIR bandpass filter with DGS (a) top and (b) bottom.

Measurement was carried out using an Agilent HP 8720B Network Analyzer. The results of S-parameter in pass band for the fabricated sample compared to the simulated results are shown in Fig. 17.

As it is observed in Fig. 17, insertion loss of the fabricated model is 2.6 dB at the center frequency, which is about 1 dB higher than the simulation results. In addition, return loss of the fabricated model is 20 dB, which is close to simulation results, as seen in Fig. 17.
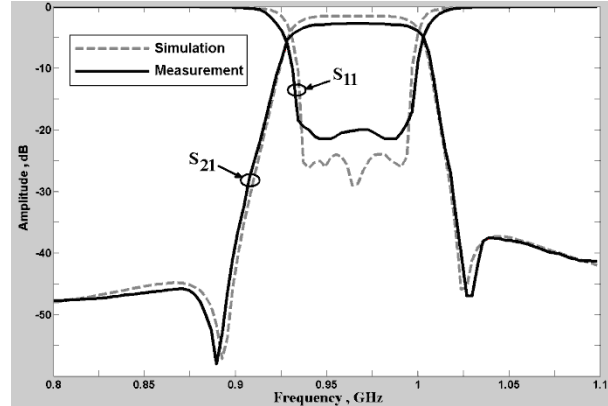

Fig. 17. Measured and simulated results of S-parameter response in pass band.

The measured sample presented a good response in rejection band, as illustrated in Fig. 18. By comparing Fig. 18 to the simulation result (Fig. 15), we observe a good accordance between them.
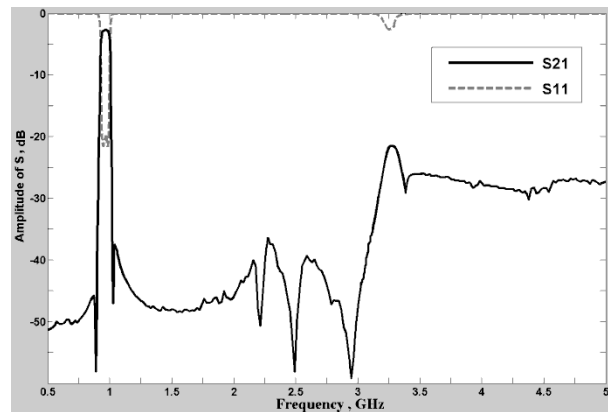

Fig. 18. Measured results in rejection band width.

IV. CONCLUSION

We have designed and fabricated a microstrip quasi-elliptic four-pole cross-coupled FTSIR filter for one of the GSM frequency bands, which may be used in further communication applications. The folded tri-section SIR not only makes the resonator more compact, but also enables the

flexibility of introducing cross coupling in a filter configuration. A comprehensive treatment of a capacitively loaded transmission line resonator is described, which leads us to apply a microstrip folded tri-section stepped impedance resonator. By etching five simple linear slots in the ground plane, we have obtained a great improvement in elimination of the first spurious resonant frequency. The measured results in the pass band and rejection band are in a good agreement with the simulated ones.

REFERENCES

[1] N. Molaei Garmjani and N. Komjani, "Quasi-Elliptic Bandpass Filter Based on SIR With Elimination of First Spurious Response," *Progress In Electromagnetics Research C*, vol. 9, pp. 89-100, 2009.

[2] J. S. Hong and M. J. Lancaster, *Microwave Filters for RF/Microwave Applications*, John Wiley & Sons, 2001.

[3] J. S. Hong and M. J. Lancaster, "Theory and experiment of novel microstrip slow-wave open-loop resonator filters," *IEEE Trans. on Microwave Theory and Tech.,* vol. 45, no. 12, December, 1997.

[4] R. Levy, "Filters with single transmission zeros at real or imaginary frequencies," *IEEE Trans. Microwave Theory Tech.*, vol. MTT-24, pp. 172-181, 1976.

[5] A. Abdel-Rahman, A. K. Verma, A. Boutejdar, and A. S. Omar, "Compact Stub Type Microstrip Bandpass Filter Using Defected Ground Plane, " *IEEE Microwave and Wireless Components Letters*, vol. 14, no. 4, April, 2004.

[6] R. K. Hoffmann, *Handbook of Microwave Integrated Circuits*, Artech House, Norwood, 1987.

[7] D. Ahn, J. S. Park, C. S. Kim, J. Kim, Y. Qian, and T. Itoh, "A Design of the Low-pass Filter using the Novel Microstrip Defected Ground Structure, " *IEEE Trans. Microwave Theory Tech*., vol. 49, no. 1, Jan, 2001.

[8] P. Vágner and M. Kasal, "Bandpass Filter Design Using an Open-Loop Defected Ground Structure Resonator," *15th Conference on Microwave Tech.,* Brno, Czech Republic, 2010.

Nima Molaei Garmjani was born in Tehran, Iran, in 1982. He received the B.S. degree in Electrical Engineering from Azad University, Iran, in 2006, the M.S. degree in Communication Engineering from Iran University of Science and Technology, Tehran, Iran, in 2009. His research interests include the design and analysis of microwave bandpass filter circuits and microstrip stepped impedance resonators (SIR).

Nader Komjani was born in Tehran, Iran, in 1965. He received the B.S., M.S. and Ph.D. degrees in Communication Engineering from Iran University of Science and Technology in 1988, 1991 and 2000, respectively. From 1991 to 1994, he joined the Iranian Science Organization of Science and Technology. His current research interests are in phased array antennas, UWB and multi-band microstrip antenna, and numerical methods in electromagnetic. Currently, he is associated professor and the Director of the Antenna Lab. in the Electrical Engineering Department, Iran University of Science and Technology.